Thioflavin T fluorescence and NMR spectroscopy suggesting a non-G-quadruplex structure for a sodium binding aptamer embedded in DNAzymes

Runjhun Saran[1,2,#], Kyle A. Piccolo[1,#], Yanping He[1,2,3,#], Yongqiang Kang[4], Po-Jung Jimmy Huang[1,2], Chunying Wei[4], Da Chen[3], Thorsten Dieckmann[1,*] and Juewen Liu[1,2,*]

[1] Department of Chemistry [2] Waterloo Institute for Nanotechnology, University of Waterloo, Waterloo, Ontario, N2L 3G1, Canada; rsaran@uwaterloo.ca (R.S.); kyle.piccolo@uwaterloo.ca (K.P.); p8huang@uwaterloo.ca (P.H.) thorsten.dieckmann@uwaterloo.ca (T.D.); liujw@uwaterloo.ca (J.L.)

[3] State Key Laboratory of Precision Measurement Technology and, Instruments, Tianjin University, Tianjin, 300072 P.R. China; heyanping@ahnu.edu.cn (Y.H.); dachen@tju.edu.cn (D.C.)

[4] Key Laboratory of Chemical Biology and Molecular Engineering of Ministry of Education, Institute of Molecular Science, Shanxi University, Taiyuan, 030006, P.R. China; y57kang@uwaterloo.ca (Y.K.) weichuny@sxu.edu.cn (C.W.)

[#] R.S. Y.H. and K.A.P. contributed equally to this work.

[*] Correspondence: thorsten.dieckmann@uwaterloo.ca (T.D.); liujw@uwaterloo.ca (J.L)

Abstract: Recently, a Na^+-binding aptamer was reported to be embedded in a few RNA-cleaving DNAzymes including NaA43, Ce13d and NaH1. These DNAzymes require Na^+ for activity but show no activity in the presence of K^+ or other metal ions. Given that DNA can selectively bind K^+ by forming a G-quadruplex structure, this work aims to answer whether this Na^+ aptamer also uses a G-quadruplex to bind Na^+. The Na^+ aptamer embedded in Ce13d consists of multiple GG sequences, which is also a pre-requisite for the formation of G4 structures. To delineate the structural differences and similarities between Ce13d and G-quadruplex in terms of metal binding, thioflavin T (ThT) fluorescence spectroscopy, NMR spectroscopy and CD spectroscopy were used. Through comparative ThT fluorescence spectrometry studies, we deciphered that while a control G-quadruplex DNA exhibited notable fluorescence enhancement up to 5 mM K^+ with a K_d of 0.52 mM, the Ce13d DNAzyme fluorescence was negligibly perturbed with similar concentrations of K^+. Opposed to this, Ce13d displayed specific remarkable fluorescence decrease with low millimolar concentrations of Na^+. NMR experiments at two different pH values suggest that Ce13d adopts a significantly different conformation or equilibrium of conformations in the presence of Na^+ versus K^+ and has a more stable structure in the presence of Na^+. Additionally, absence of characteristic peaks expected for a G-quadruplex structure in 1D ^1H NMR suggest that G4 is not responsible for the Na^+ binding. This theory is confirmed by absence of characteristic peaks in the CD spectra of this sequence. Therefore, we concluded that the aptamer must be selective for Na^+ and binds using a structural element that does not contain G4.

Keywords: aptamers; DNAzymes; sodium; fluorescence; NMR.

https://doi.org/10.1139/cjc-2021-0024
https://cdnsciencepub.com/doi/10.1139/cjc-2021-0024

1. Introduction

Understanding of metal-binding to DNA is important not only for studying the biological functions of DNA, but also for biosensor development, [1, 2] drug development, [3] and nanotechnology. [4] In biological studies, Na^+ and K^+ are among the most abundant physiological metal ions. They can control the ionic strength of buffers and solutions and screen the negative charges on DNA, resulting in more stable DNA duplexes. [5] In addition, they can also have specific binding interactions with certain single-stranded DNA sequences. [1] The most famous example is of the stabilization of G-quadruplex (G4) DNA. [6] Normally K^+ is much more effective than Na^+ in stabilizing G4 structures. [7, 8] Na^+ is less effective often attributed to its smaller size and also because thermodynamically it has a higher energy of dehydration. [8]

Recently, a Na^+-binding DNA aptamer has been reported, [9, 10] which was derived from the conserved sequences of the DNAzymes NaA43, NaH1, and Ce13d all originally discovered through *in-vitro* selections. [11, 12, 13, 14] The NaA43 DNAzyme was reported by Lu and coworkers, [11] and it specifically requires Na^+ for cleaving an RNA containing substrate. NaA43 shares its conserved sequence with the Ce13d DNAzyme, which was selected by our group in a lanthanide-dependent selection. [12] The conserved sequence is the main part of a Na^+-binding aptamer. [15, 16, 17, 18] The identification of this Na^+-aptamer proved instrumental in understanding the reason for the specificity of NaA43 and Ce13d DNAzymes for Na^+, although the mechanism underlying specific Na^+ binding by the DNA still remains intriguing. [10, 17, 19, 20] Our knowledge on specific Na^+ binding by DNA is limited and from the literature known, and a possible mechanism may rely on G4 structures. In such a case, the G4 structure would require a superior Na^+-induced stabilization than K^+, as the aptamer is known to show a higher affinity to Na^+ in comparison to K^+ especially at room temperature. [9, 16, 19, 21] Outside the G4 context, Na^+ binds more strongly to DNA than K^+ since it can better increase the melting temperature (T_m) of DNA. [22] With respect to G4 structures, so far only a few specialized examples are known where Na^+ can stabilize G4 more than K^+ does. Alberti and coworkers reported a structure containing two contiguous G4 units with a greater stabilization by Na^+. [23] Other examples of Na^+ being a better stabilizer were all from mutated human telomeric sequences, but the advantage of Na^+ was extremely small. For example, by replacing a certain guanine with a O^6-methylguanines, the T_m was enhanced by just 1 °C with Na^+, while the T_m of the original DNA was 8 °C higher with K^+. [24] Moderate advantages were also observed by replacing certain guanines by abasic sites, [25] or adenines. [26] Overall, such mutations significantly decreased the overall stability of the G4 structures. For unmodified simple G4 sequences, no examples are known for Na^+ being a better stabilizer. Therefore, it would be extremely intriguing to probe whether the mechanism underlying Na^+-binding to the aptamer derived from NaA43 and Ce13d DNAzymes involves Na^+-G4 interactions.

Thioflavin T is a popular dye that becomes fluorescent upon binding to G4 DNA, and it has been extensively used to probe G4. [27] In addition, NMR is a powerful method for studying G4 structures. [28, 29] In this work, we used ThT to study Na^+ binding by the Ce13d DNAzyme and a comparison was made with a G4 structure. In addition, NMR spectroscopy was performed to further analyze the Ce13d DNAzyme structure. The results argued against the presence of a G4 structure to be responsible for the specific Na^+ binding by the aptamer.

2. Results and Discussion

2.1. The Ce13d DNAzyme

The secondary structure of the Ce13d DNAzyme is shown in Figure 1A. [12] Its substrate strand contains a single RNA linkage (rA in red for ribo-adenine) that serves as the cleavage site. For most of the studies in this work, this RNA linkage was replaced by its DNA analog to avoid cleavage. Previous assays have shown that such a change does not perturb Na^+ binding. [9, 21] The enzyme strand binds the substrate via two stems (shown as blue/green duplexes in Figure 1A), and the enzyme contains a large loop between the two stems which is the main part of the Na^+ aptamer (shown as red and yellow). G4 structures are composed of stacked G-quartet, where each quartet consists of 4 guanines Hoogsteen base paired in a square planar array (Figure 1D). G4s may form by

one to four nucleic acid strands that bear continuous runs of guanines or G-tracts in presence of metal ions such as K^+. [30, 31]

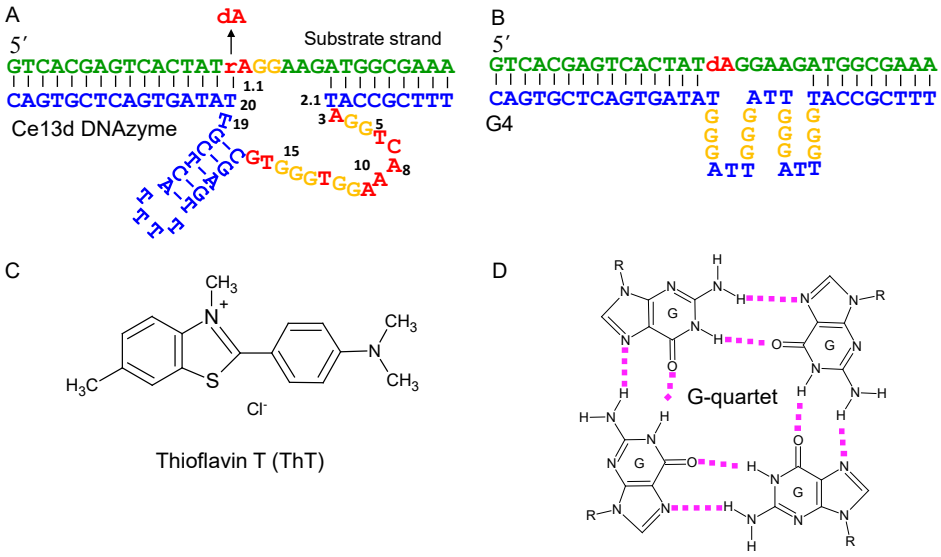

Figure 1. The secondary structure of (A) the Ce13d DNAzyme and (B) G4 construct, designed by replacing the Ce13d catalytic loop by a G4 DNA. The guanine stretches are marked in yellow. (C) The structure of ThT. (D) Structural representation of a G-quartet, where the hydrogen bonds are shown in pink color, G stands for guanine, and R depicts the rest of the nucleic acid chain attached to G.

From the secondary structure of Ce13d, we can find four GG or GGG stretches (yellow, Figure 1A) in its catalytic loop, and thus it has the chemical components to form a G4. From the previously published DMS foot-printing experiment, most of these guanines in the enzyme strand were protected in presence of Na^+, indicating that these guanines are involved in the Na^+-binding pocket. [9] However, this DNAzyme is known to be inactive with K^+. [19] In addition, upon replacing one of the critical guanines in the enzyme catalytic loop with base hypoxanthine, the modified Ce13d DNAzyme still retained the same Na^+-induced activity. [32] This modification must disrupt G4 structures, however it did not hamper the Ce13d activity. Therefore, whether Ce13d uses G4 to bind Na^+ remains elusive. To address this problem through comparative studies, we designed a G4 construct as a positive control, in which we replaced the Ce13d catalytic loop with a G4 sequence (Figure 1B).

2.2. ThT fluorescence spectroscopy

We started by using ThT to probe for the presence of G4 structures in the Ce13d DNAzyme and the G4 control sequence. The structure of ThT is shown in Figure 1C, and it is commonly used for staining G4 DNA. [27, 33, 34, 35] ThT prefers to bind parallel G-quadruplex over anti-parallel ones. [36, 37] Before studying our Ce13d DNAzyme, we first did a control experiment using the G4 construct in Figure 1B. We mixed ThT with this G4 structure and an emission peak at 488 nm was observed with 442 nm excitation (Figure 2A, black spectrum). Upon adding 10 mM K^+, an increase in the fluorescence was observed, suggesting formation of a G4 structure (Figure 2A, red spectrum). For quantitative understanding, we gradually titrated K^+ (Figure 2B, green trace) to see a concentration-dependent effect. A sharp increase in fluorescence occurred between 0 and 5 mM K^+ and then the fluorescence saturated. A K_d of 0.52 mM K^+ was obtained by fitting the curve. With more than 10 mM K^+, the fluorescence started to drop, which might be attributed to the general effect of salt in screening the interaction between ThT and the DNA. While the increase in fluorescence in Figure 2B was sharp, it was relatively small in terms of fold-enhancement i.e. ~ 2-fold. This could be attributed to the long DNA structure in which only a small fraction of the nucleotides makes the G4 structure. The non-guanine nucleotides may non-specifically bind ThT and thus may have contributed to a high background fluorescence. [35] In addition, this G4 DNA might fold into an anti-parallel structure,

which would also limit the amount of fluorescence increase (see discussion on its CD spectra later). When Li^+ was titrated, no fluorescence increase was observed and it even dropped slightly (Figure 2B, black trace). When Na^+ was titrated, the drop in fluorescence was even more (Figure 2B, red trace). Overall, the control G4 experiment indicated that ThT can stain the G4 structure in our two-strand system (Figure 1B), and only K^+ promoted formation of the G4 structure.

We then titrated the metal ions to the Ce13d DNAzyme containing the non-cleavable substrate (Figure 2C). Interestingly, we observed decreased fluorescence intensity upon addition of Na^+, while K^+ almost had no influence on the signal, similar to the response to Li^+. This data indicates that Na^+ binding made the structure less like a G4. We reason that Na^+ can fold the DNAzyme into a tight binding structure, releasing previously associated ThT to decrease its fluorescence. , To ensure that the data is representative, we also performed the metal titration in the presence of a lower buffer concentration (Figure S1). Still, Na^+ showed the largest ThT fluorescence decrease, confirming specific Na^+-binding but likely to a non-G4 structure.

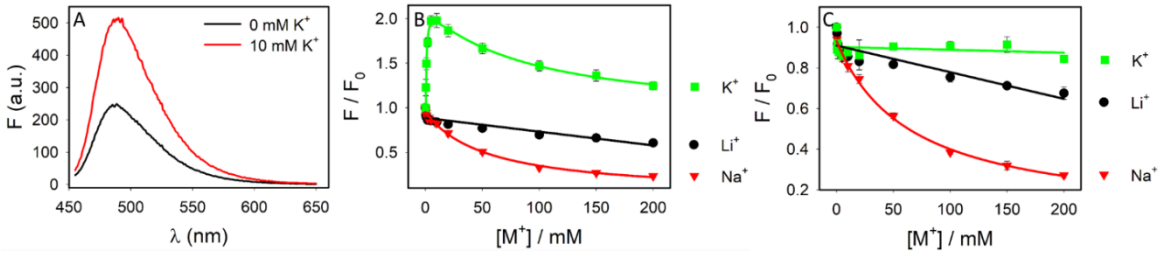

Figure 2. (A) Fluorescence spectra of the G4/ThT mixture without and with 10 mM K^+. Fluorescence titration of the (B) G4/ThT, and (C) Ce13d/ThT mixture with various monovalent metal ions in 500 mM Tris-acetate buffer, pH 8.0.

Another possibility is of the formation of inter-molecular G4 complexes by multiple DNAzymes specifically interacting with each other. To test this, we varied the concentration of the Ce13d DNAzyme (keeping the ThT concentration the same). As we increased the concentration of DNAzyme, the initial fluorescence increased, which is consistent with formation of increasing DNA/ThT complexes. However, this response to Na^+ was observed to be independent of DNAzyme concentration, upon plotting the relative fluorescence change (Figure S2). This data advocate that the effect of the Na^+-binding is conferred upon individual DNAzyme molecules rather than the formation of inter-molecular complexes.

An important aspect of ThT staining to be considered is the possibility of G4-induced fluorescence reduction. It has been previously reported that using ThT to stain G4 DNA followed by addition of metal ions may not always accompany fluorescence increase, and sometimes fluorescence decrease may also be observed. [27] Based on the available literature, in most common cases with unmodified DNA we expect K^+ to be better than Na^+ to stabilize G4 structures, although exceptions were also reported. [38, 39] The fact that only Na^+ had a strong response of decreasing fluorescence with negligible fluorescence perturbation in presence of K^+ (Figure 2C) did not provide a strong support for a G4 structure in Ce13d with Na^+. The insights from previous 2-aminopurine spectroscopy studies, [19] in addition to the data fished out in our study herein, strengthen the notion of Ce13d DNAzyme to fold differently than G4 structures in presence of Na^+. Since ThT has its limitations, the data presented here alone cannot conclude the structure of the Ce13d DNAzyme in the presence of Na^+. Therefore, we then used spectroscopic methods that do not require labeling or staining of the DNA.

2.3. Design of a cis-DNAzyme for NMR spectroscopy

To further confirm our results, we performed NMR spectroscopy. One of the main bottlenecks in obtaining information from nucleic acid NMR is the length of the sequence under study. The chemical diversity of the nucleotide monomers (i.e. adenine, thymine/uracil, cytosine, and guanine)

present in naturally occurring nucleic acids is very low. Due to this there is high spectral overlap in their NMR peaks. [40] This problem becomes more and more significant as the number of nucleic acid polymers or the number of nucleotides increase. [41] The DNAzyme version used for ThT experiments (Figure 1A) contains two separate strands, and the full Ce13d DNAzyme used for previous studies had nearly 90 nucleotides. It is difficult to prepare a homogenous NMR sample with the two-strand system, since it is hard to control the presence of any unhybridized strand by having exactly the same ratio of the two strands. Such heterogeneity adds spectral overlap of NMR peaks as well, making NMR analysis even more difficult. Therefore, to lessen the probability of spectral overlap, short cis versions of Ce13d were designed for NMR studies.

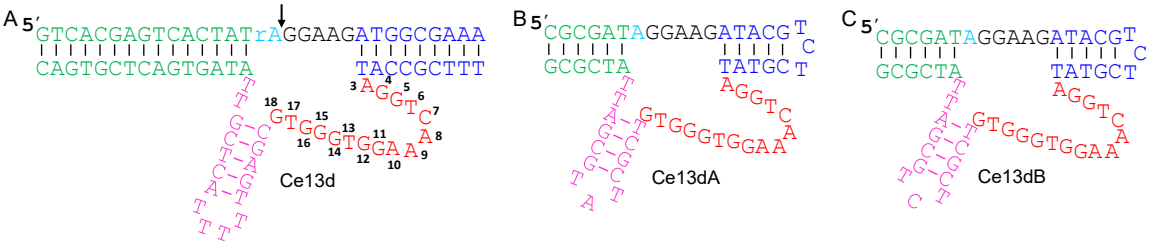

Figure 3. The secondary structure of (A) trans-cleaving DNAzyme Ce13d with the conserved nucleotides (red) numbered from 3-18, and its non-cleavable analogues (B) Ce13dA, and (C) Ce13dB.

The secondary structure of the trans-cleaving Ce13d previously used for biochemical characterizations, [32] and the two short cis versions: Ce13dA and Ce13dB used for NMR studies are shown in Figure 3. The two substrate binding arms of these two cis DNAzymes are 6 base pair (shown in green color) and 5 base pair (shown in blue color) long, much shorter than those in Ce13d. Previous studies showed that the hairpin size and composition can be change as long as a hairpin structure is retained. [12, 16, 19] In the catalytic loop, the length of the hairpin was also shortened. The only difference between Ce13dA and Ce13dB is that the adenine in the tip of the hairpin loop was changed to a cytosine. Shortened cis-DNAzymes were used to solve the DNA length and substrate/enzyme ratio problems. The region shown in dark red is the same for all three versions shown. These conserved nucleotides present in the enzyme loop of Ce13d are most important for Na^+-binding as well as catalytic activity (nucleotides numbered 3-18 in Figure 3 A). A systematic mutation study of the conserved enzyme loop, in which each nucleotide was mutated to the other three has revealed interesting insights. [16] It was found that most of the mutants except for A3G, A8G, G14A, and G14T, were incapable of specific Na^+-binding. In terms of catalytic activity, the nucleotides A3, G14 and T17 exhibited tolerance to mutations, and mutants C7A, A8G, and T13C were found active. Except these, all the other mutants remarkably hampered the Ce13d catalysis. These data present a good correlation between Na^+-binding and catalytic activity, showing that Na^+-binding is a key factor for catalysis to take place. These data also validate the usage of Ce13dA and Ce13dB for NMR, as these have the conserved set of nucleotides preserved. In the trans-cleaving Ce13d DNAzyme (Figure 3 A), the cleavage site is denoted with a black arrow, and the cleavage site ribonucleotide 'rA' is colored in cyan. The cis-versions of Ce13d are designed to be non-cleavable by replacing the cleavage site 'rA' to deoxy-ribonucleotide 'A' (colored in cyan in Figure 3B and 3C).

2.4. Folding of Ce13d in Li^+, Na^+ and K^+.

To see if we could gain a deeper understanding of the folding of Ce13d in the presence of various monovalent ions we probed the 1D ^1H spectrum of Ce13dA in the presence of various monovalent ions at two different pH values (Figures 4 and 5). The imino proton regions of 90% H_2O/10% D_2O 1D ^1H NMR spectra of Ce13dA were collected with no salt added (only trace amounts of Li^+ present) at pH 6.8 (Figure 4A), 10 mM K^+ at pH 6.8 (Figure 4B), and 10 mM Na^+ at pH 6.8 (Figure 4C) respectively. The imino region of the 1D ^1H spectrum contains peaks for the exchangeable imino protons of guanine (H1) and thymine (H3). [42] More specifically, the region of 12-14 ppm represents signals

from imino (NH) protons which are strongly hydrogen bonded in Watson-Crick base pairs, while the signals in the region around 9-12 ppm belong to imino protons that are typically involved in non-canonical base pairs which are useful for characterizing the secondary structures formed by complexed DNA. [43, 44] A comparison of the three spectra in the region of 12-14 ppm in Figure 4 suggests that there are similar number of peaks and several shared chemical shifts between each of the three spectra, suggesting that the structure of the base paired regions shown in Figure 3B was relatively rigid and stable in the presence of traces of Li^+, or 10 mM Na^+, and K^+ at pH 6.8. However, the region of 9-12 ppm is quite different with respect to the number of peaks and chemical shifts of the peaks for each of the three spectra, indicating that Ce13dA adopted a different conformation and/or equilibrium of conformations in the presence of no salt (Li^+ traces), Na^+ and K^+.

In Figure 5, similar spectra were acquired but at a lower pH of 5.8 and with higher salt concentrations of 80 mM K^+ (Figure 5B) and 80 mM Na^+ (Figure 5C) to drive the binding of the cations. Under these conditions, the spectra for Li^+ and K^+ had a much broader linewidth and more spectral overlap, resulting in poorly defined peaks. This is indicative of the presence of multiple conformations, which is unsurprising at a lower pH where exchange occurs more readily due to higher H^+ concentration. On the other hand, it can be observed in Figure 5C that there are shifts in the Na^+ spectrum from higher salt concentration and lower pH, but in general it retains its structured conformation. From Figure 4, it is evident that many of the peaks affected in presence of Na^+ are different from those affected with K^+, and at the lower pH of 5.8 where the exchange rate is higher, Ce13dA visibly retains much more structure in the presence of Na^+ than the free DNA or in the presence of K^+. This emphasizes that Ce13dA adopts a different conformation and/or equilibrium of conformations in the presence of Na^+ versus K^+. It is also worth noting that in Figure 4, there are fewer peaks present in the absence of salt than there are in the presence of Na^+ or K^+ which implies that some features of the folded structures are unable to form without cation stabilization. These interpretations support the conclusions of previous results, where using intrinsic fluorescence changes of 2-aminopurine labeled at the cleavage site, it was shown that the folding pattern with Na^+-binding was completely different from K^+-binding, where K^+ is considered to induce misfolding of Ce13d. [19, 21]

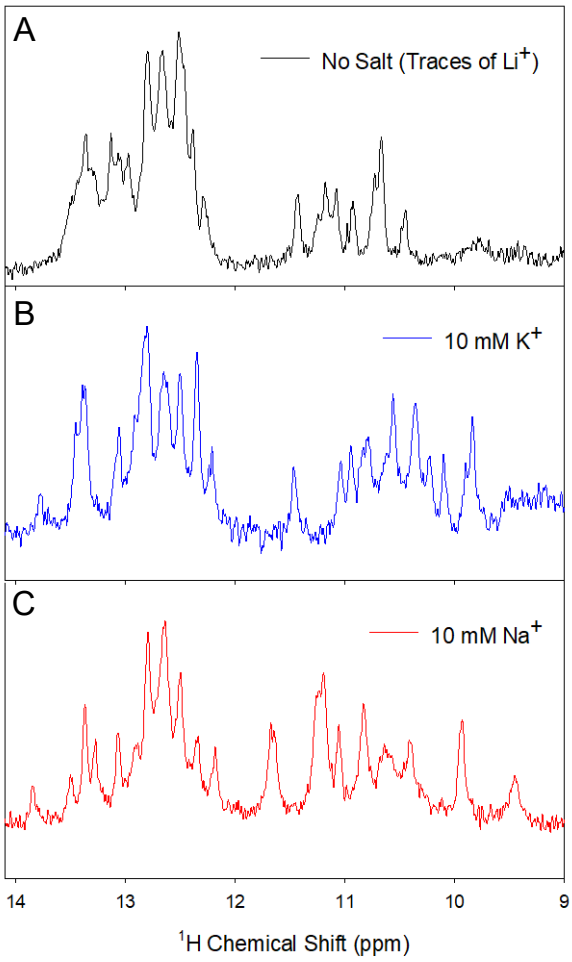

Figure 4. Imino proton region of 90 % H_2O / 10 % D_2O 1D ^1H NMR spectra of Ce13dA at 277K. (A) 600 µM Ce13dA with no salt added (only trace amounts of Li^+ from purification present), pH 6.8, (B) 150 µM Ce13dA in 10mM K^+, pH 6.8, (C) 150µM Ce13dA in 10mM Na^+, pH 6.8.

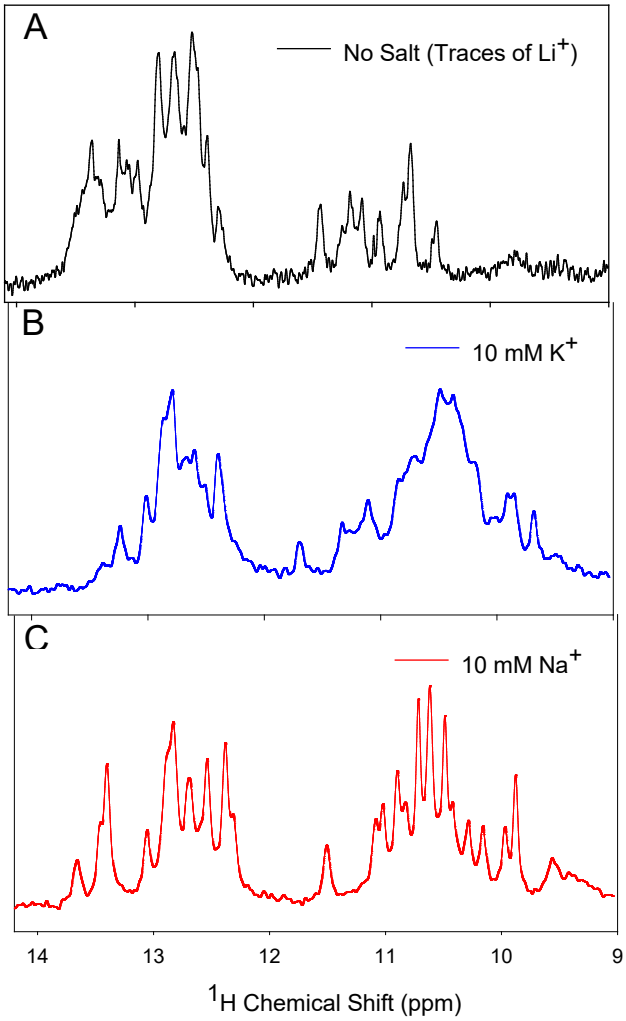

Figure 5. Imino proton region of 90 % H_2O / 10 % D_2O 1D ^1H NMR spectra of Ce13dA at 277K. (A) 150 µM Ce13dA with no salt added (only trace amounts of Li^+ from purification present), pH 5.8, (B) 150 µM Ce13dA in 80mM K^+, pH 5.8, (C) 150µM Ce13dA in 80mM Na^+, pH 5.8.

2.5. NMR spectra suggest the Na^+-binding structure is not a G-quadruplex.

Many G-rich DNA aptamers contain G-quadruplex structures for molecular recognition, and these structures have fairly well defined guanine imino ^1H NMR shifts between 10.5-12.5 ppm. [45, 46, 47, 48] G-quadruplex DNA is a highly stable structure and therefore these peaks are typically defined by high intensity and narrow linewidth. Due to the Na^+ dependence of the Ce13d DNAzyme and its sequence containing sufficient G-rich regions, NMR was also used to qualitatively assess the presence of G-quadruplex DNA. This needed the investigation of Ce13d in presence of Na^+ due to its functional role, and also in presence of K^+ because of the well-established preference of G-tetrads for K^+. [49, 50] The spectra in Figures 4 and 5 were analyzed for this purpose. However, no compelling evidence supported the presence of a G-quadruplex in Ce13dA in the presence of Na^+ or K There are some peaks between 10.5 ppm and 12.5 ppm at both pH ranges but this is not atypical of DNA, and based on the linewidths, G-quadruplex is not conclusively present in any of the spectra. At pH 5.8, it is highly likely that a G-quadruplex would be stable and retain its characteristic, narrow imino peaks between 10.5-12.5 ppm and it is clear that this is not the case for free DNA or in the presence of K^+. In the presence of Na^+, peaks in this region are much sharper but located in the same region. Analysis of Figure 4 shows that there are not significantly more peaks in the presence of Na^+ than K^+. Based on these observations and the fact K^+ is known to have a higher propensity for G-quadruplex formation than Na^+, it is unlikely that Ce13dA forms a G-quadruplex. Additional evidence against the presence of G-quadruplex was acquired by running D_2O spectra with the three samples from Figure 5. These

samples were lyophilized after the previous spectra were obtained, resuspended in D_2O and spectra were acquired within 30 minutes of resuspension. Under these conditions, signals from exchangeable imino and amino resonances from G-quadruplex G residues may survive for up to two or more weeks in D_2O. [51] To summarize, these ^1H NMR spectra support the presence of a specific and unique aptamer for Na^+ within the catalytic loop of Ce13d and show that this aptamer is not based on a G-quadruplex structure.

2.6. CD spectra confirm the absence of G-quadruplex structure.

CD spectra were then obtained for Ce13dA under the same three salt conditions used for NMR experiments (no salt added, 80 mM K^+ and 80 mM K^+). We chose the cis-cleaving Ce13dA to better match the results of the NMR experiments. All three spectra had maxima at approximately 280 nm, minima at 250 nm and a cross-over point from positive to negative intensity around 260 nm which is typical of duplex DNA (Figure S5). [52, 53] G-quadruplex DNA can have different forms, all with characteristic CD signatures, such as parallel (~264 nm max, 245 nm min), antiparallel (~ 295 max, 260 min) or hybrid (~ 295 max, 260 max, 245 min). [54, 55] These peaks are clearly not present in any of the CD spectra obtained. In addition to this, all three salt conditions give nearly identical CD spectra, which is not consistent with the presence of a G-quadruplex. Since G-quadruplex formation is dependent on salt, a sequence containing G-quadruplex would experience significant shifts in wavelengths and increases in peak magnitudes in the presence of K^+ compared to the absence of K^+. [56] We previously measured the CD spectra of the trans-cleaving Ce13d DNAzyme and also the G-quadruplex control shown in Figure 1A and 1B, respectively [20]. The trans-cleaving Ce13d spectra were very similar to that of the cis-cleaving Ce13dA presented in Figure S5, suggesting that they had a similar overall folding. The G4 control, on the other hand, had the peaks shifted to 290 nm and 250 nm in the presence of K^+, suggesting its folding into an anti-parallel G-quadruplex. The peaks did not perfectly match with the ideal values since a portion of the DNA was in duplex. This evidence indicates that Ce13dA does not form a G-quadruplex, in agreement with 1D NMR data.

2.7. Potential Structural Information from 2D NMR

In addition to the 1D ^1H NMR, we probed the structure of Ce13d with 2D NMR. For this we used the Ce13dB construct. The Ce13dB differs from Ce13dA by a cytosine residue its hairpin-loop (shown in pink in Figure 3B and 3C). This change could be afforded as this position is known to be insignificant in Na^+ binding and catalysis of Ce13d. [12, 32] This was done to increase the number of cytosine residues as it proves beneficial for spectral assignment of peaks, and therefore in determining the homogeneity of the sample. Typically for cytosines, the H5 and H6 protons show up peaks between 5-6 ppm and 6.9-7.9 ppm respectively. The through-bond interaction between H5 and H6 protons is unique to cytosines, and the number of peaks coming from this interaction directly correlates to the number of cytosines in the structure. To determine if Ce13dB is present in a single homogeneous conformation, we probed the structure of Ce13dB with a 2D TOCSY experiment (Figure S3), and looked at the peaks generated by the through-bond interactions of H5/H6 protons in the cytosine nucleotides (Figure S4). The number of cytosines in Ce13dB is 12 (Figure 1 C), while the number of peaks showing up in the 100 % D_2O $^1H5/^1H6$ 2D TOCSY is 18 (Figure S4). This clearly indicated that Ce13dB is present in multiple three-dimensional conformations. Since conformational homogeneity is a pre-requisite for structure determination through NMR, any further spectra for structure determination was not acquired this study.

3. Materials and Methods

3.1. Chemicals

The DNA sequences were obtained from Integrated DNA Technologies (Coralville, IA) and Eurofins (Huntsville, AL). Metal salts including lithium chloride (LiCl), sodium chloride (NaCl), KH_2PO_4, K_2HPO_4, Na_2HPO_4, and NaH_2PO_4 were obtained from Sigma-Aldrich, VWR, and Fischer Scientific Canada at the highest purity available. ThT was from Sigma-Aldrich. 99.9% D_2O was from Cambridge Isotope Laboratories.

3.2. ThT fluorescence spectroscopy

For ThT fluorescence spectroscopy, the Ce13d DNAzyme or G4 complexes were annealed at a final concentration of 20 μM in buffer A (25 mM LiCl, 50 mM HEPES, pH 7.5) by heating the samples to 85 °C for 5 min and then gradually cooling to 4 °C over 30 min. For the experiments, final concentration of 0.6 μM DNA complexes were added to a final concentration of 3 μM ThT solution in buffer B at room temperature (500 mM TA, pH 8). After 15 min reaction at 4°C, the sample was recovered to room temperature. Then fluorescence readings were collected on a Cary Eclipse fluorometer in a 1x1 cm quartz fluorescence cuvette with the excitation wavelength (λ_{exc}) as 442 nm and the scanning emission wavelength (λ_{emm}) range from 455 to 650 nm at room temperature.

3.3. Nuclear Magnetic Resonance

DNA for NMR experiments was purified by 10% denaturing polyacrylamide gel electrophoresis (dPAGE). The DNA was eluted from the dPAGE using 300 mM LiCl. This was followed by purification on a HiPrep 16/10 DEAE FF anion-exchange column (GE Healthcare, Uppsala, Sweden), and desalting on a HiPrep 26/10 Desalting column (GE Healthcare, Uppsala, Sweden). Buffers containing only Li^+ cations (no Na^+ or K^+) were used throughout purification. NMR samples were prepared by dissolving an appropriate weight of lyophilized powder in 400μL of either water (no salt samples), 5 mM NaH_2PO_4 and 5 mM NaCl, 5 mM KH_2PO_4 and 5 mM KCl, 80 mM NaCl or 80 mM KCl. The pH was adjusted to 5.8 or 6.8 with ammonia, NaOH or KOH depending on the cation already present. The samples were dried by lyophilization and re-dissolved in 500 μL of 90% H_20/10% D_2O or 99.9% D_2O. Samples were heated to 85°C for 5min and cooled to 4°C before spectra were acquired. All spectra were collected on a Bruker DRX-600 spectrometer equipped with a HCN triple-resonance, triple-axis PFG probe (Bruker, Billerica, MA). ^1H NMR experiments were carried out at 277 K in 90% H_2O/10% D_2O or 298 K in D_2O. Solvent suppression was achieved using 1-1-spin echo pulse sequences [57] for 90% H_2O/10% D_2O or presaturation [58] for D_2O samples.

The 2D CITY TOCSY [59] experiment was run at 298 K in 100% D_2O. and quadrature detection for the indirect dimension was achieved using the States-TPPI method. [60]

3.4. Circular Dichroism

CD experiments were performed on a Jasco J-815 spectropolarimeter (Jasco Inc., Easton, MD). CD scanning experiments were run from 330 nm to 200 nm with a path length of 0.1 cm, data interval of 0.5 nm, band width of 0.5 nm, response of 1 second, scanning speed of 200 nm minute−1 and a total of four accumulated scans. Samples contained 5 μM DNA at pH 6.8 and either H_2O, 80 mM KCl or 80 mM NaCl. The samples were also heated to 85 °C for 5min, cooled to 4 °C and incubated for at least 24hrs before acquisition at 25 °C.

4. Conclusions

In this study, ThT staining, NMR spectroscopy and CD spectroscopy were employed to study Na^+ binding by its aptamer, which is embedded in the Ce13d and NaA43 DNAzymes. By accomplishing comparative analysis between Ce13d Na^+-aptamer versus a G4 construct, it was observed that both show a distinct fluorescence change in the presence of Li^+, Na^+ and K^+. In case of Ce13d, while most of the binding was observed with Na^+, no evidence supported that formation of a G4 structure makes the basis of Na^+-binding, and thus this aptamer likely uses other mechanisms to bind Na^+. NMR provided a similar conclusion arguing against a G4 structure in the presence of Na^+. This is further supported by lack of G4 observed in CD. This report not only explicitly demonstrates the presence of a uniquely folding novel Na^+-aptamer in Ce13d, but also substantiates that fact that isolation of novel aptamer containing DNAzymes or Aptazymes are a prudent way of discovering novel distinctly folding metal-binding aptamers. Additionally, this study highlights the possibility of utilizing monovalent metal ions to play novel and unique roles in DNA scaffolding and DNA nanotechnology in general, other than just nucleic acid duplex stabilization.

Supplementary Materials: The following are available online at www.mdpi.com/xxx/s1, Figure S1. Fluorescence intensity in lower buffer concentration, Figure S2. Fluorescence intensity at different DNA concentrations, Figure S3. 2D-TOCSY spectrum of 450 μM Ce13dB in 5 mM $LiPO_4$ pH 6.8, 200 mM Na^+, Figure S4. H5/H6 proton region of the 2D-TOCSY spectrum of Ce13dB.

Funding: This research was funded by the Natural Sciences and Engineering Research Council of Canada (NSERC). Y. He was supported by China Scholarship Council (CSC) and Y. Kang was supported by a scholarship from Shanxi University to visit the University of Waterloo.

Conflicts of Interest: The authors declare no conflict of interest.

References

1. Zhou, W.; Saran, R.; Liu, J. Metal Sensing by DNA. *Chem. Rev.* **2017**, *117*, 8272–8325.
2. Zhang, X.-B.; Kong, R.-M.; Lu, Y. Metal Ion Sensors Based on DNAzymes and Related DNA Molecules. *Annual Review of Analytical Chemistry* **2011**, *4*, 105-128.
3. Jamieson, E.R.; Lippard, S.J. Structure, recognition, and processing of cisplatin-DNA adducts. *Chem. Rev.* **1999**, *99*, 2467-2498.
4. Oh, T.; Park, S.S.; Mirkin, C.A. Stabilization of Colloidal Crystals Engineered with DNA. *Adv. Mater.* **2019**, *31*.
5. Sigel, R.K.O. Intimate Relationships between Metal Ions and Nucleic Acids. *Angew. Chem. Int. Ed.* **2007**, *46*, 654-656.
6. Largy, E.; Mergny, J.-L.; Gabelica, V. Role of Alkali Metal Ions in G-Quadruplex Nucleic Acid Structure and Stability. In *The Alkali Metal Ions: Their Role for Life*; Sigel, A.; Sigel, H.; Sigel, R. K. O., Eds.; Springer International Publishing: Cham, 2016; pp. 203-258.
7. Saccà, B.; Lacroix, L.; Mergny, J.-L. The effect of chemical modifications on the thermal stability of different G-quadruplex-forming oligonucleotides. *Nucleic Acids Res.* **2005**, *33*, 1182-1192.
8. Hud, N.V.; Smith, F.W.; Anet, F.A.L.; Feigon, J. The Selectivity for K+ versus Na+ in DNA Quadruplexes Is Dominated by Relative Free Energies of Hydration: A Thermodynamic Analysis by 1H NMR. *Biochemistry* **1996**, *35*, 15383-15390.
9. Zhou, W.; Zhang, Y.; Huang, P.-J.J.; Ding, J.; Liu, J. A DNAzyme requiring two different metal ions at two distinct sites. *Nucleic Acids Res.* **2016**, *44*, 354-363.
10. Torabi, S.-F.; Lu, Y. Identification of the Same Na+-Specific DNAzyme Motif from Two In Vitro Selections Under Different Conditions. *Journal of Molecular Evolution* **2015**, *81*, 225-234.
11. Torabi, S.-F.; Wu, P.; McGhee, C.E.; Chen, L.; Hwang, K.; Zheng, N.; Cheng, J.; Lu, Y. In vitro selection of a sodium-specific DNAzyme and its application in intracellular sensing. *Proceedings of the National Academy of Sciences* **2015**, *112*, 5903-5908.
12. Huang, P.-J.J.; Lin, J.; Cao, J.; Vazin, M.; Liu, J. Ultrasensitive DNAzyme Beacon for Lanthanides and Metal Speciation. *Anal. Chem.* **2014**, *86*, 1816-1821.
13. Ma, L.; Kartik, S.; Liu, B.; Liu, J. From general base to general acid catalysis in a sodium-specific DNAzyme by a guanine-to-adenine mutation. *Nucleic Acids Res.* **2019**, *47*, 8154–8162.
14. Ma, L.; Liu, J. An In Vitro Selected DNAzyme Mutant Highly Specific for Na+ in Slightly Acidic Conditions. *ChemBioChem* **2019**, *20*, 537-542.
15. Zhou, W.; Saran, R.; Ding, J.; Liu, J. Two Completely Different Mechanisms for Highly Specific Na+ Recognition by DNAzymes. *ChemBioChem* **2017**, *18*, 1828-1835.

16. Zhou, W.; Ding, J.; Liu, J. A Highly Selective Na+ Aptamer Dissected by Sensitized Tb3+ Luminescence. *ChemBioChem* **2016**, *17*, 1563–1570.
17. He, Y.; Zhou, Y.; Chen, D.; Liu, J. Global Folding of a Na+-Specific DNAzyme Studied by FRET. *ChemBioChem* **2019**, *20*, 385-393.
18. Admiraal, S.J.; Herschlag, D. Mapping the transition state for ATP hydrolysis: implications for enzymic catalysis. *Chem.Biol.* **1995**, *2*, 729-739.
19. He, Y.; Chen, D.; Huang, P.-J.J.; Zhou, Y.; Ma, L.; Xu, K.; Yang, R.; Liu, J. Misfolding of a DNAzyme for ultrahigh sodium selectivity over potassium. *Nucleic Acids Res.* **2018**, *46*, 10262-10271.
20. He, Y.; Chang, Y.; Chen, D.; Liu, J. Probing Local Folding Allows Robust Metal Sensing Based on a Na+-Specific DNAzyme. *ChemBioChem* **2019**, *20*, 2241-2247.
21. Zhou, W.; Ding, J.; Liu, J. A highly specific sodium aptamer probed by 2-aminopurine for robust Na+ sensing. *Nucleic Acids Res.* **2016**, *44*, 10377-10385.
22. Liu, B.; Kelly, E.Y.; Liu, J. Cation-Size-Dependent DNA Adsorption Kinetics and Packing Density on Gold Nanoparticles: An Opposite Trend. *Langmuir* **2014**, *30*, 13228-13234.
23. Saintome, C.; Amrane, S.; Mergny, J.L.; Alberti, P. The exception that confirms the rule: a higher-order telomeric G-quadruplex structure more stable in sodium than in potassium. *Nucleic Acids Res.* **2016**, *44*, 2926-2935.
24. Mekmaysy, C.S.; Petraccone, L.; Garbett, N.C.; Ragazzon, P.A.; Gray, R.; Trent, J.O.; Chaires, J.B. Effect of O6-Methylguanine on the Stability of G-Quadruplex DNA. *J. Am. Chem. Soc.* **2008**, *130*, 6710-6711.
25. Školáková, P.; Bednářová, K.; Vorlíčková, M.; Sagi, J. Quadruplexes of human telomere dG3(TTAG3)3 sequences containing guanine abasic sites. *Biochem. Biophys. Res. Commun.* **2010**, *399*, 203-208.
26. Sagi, J.; Renčiuk, D.; Tomaško, M.; Vorlíčková, M. Quadruplexes of human telomere DNA analogs designed to contain G:A:G:A, G:G:A:A, and A:A:A:A tetrads. *Biopolymers* **2010**, *93*, 880-886.
27. Yeasmin Khusbu, F.; Zhou, X.; Chen, H.; Ma, C.; Wang, K. Thioflavin T as a fluorescence probe for biosensing applications. *TrAC, Trends Anal. Chem.* **2018**, *109*, 1-18.
28. Adrian, M.; Heddi, B.; Phan, A.T. NMR spectroscopy of G-quadruplexes. *Methods* **2012**, *57*, 11-24.
29. Webba da Silva, M. NMR methods for studying quadruplex nucleic acids. *Methods* **2007**, *43*, 264-277.
30. Mergny, J.-L.; Sen, D. DNA Quadruple Helices in Nanotechnology. *Chem. Rev.* **2019**, *119*, 6290-6325.
31. Ueyama, H.; Takagi, M.; Takenaka, S. A novel potassium sensing in aqueous media with a synthetic oligonucleotide derivative. fluorescence resonance energy transfer associated with guanine quartet-potassium ion complex formation. *J. Am. Chem. Soc.* **2002**, *124*, 14286-14287.
32. Vazin, M.; Huang, P.-J.J.; Matuszek, Ż.; Liu, J. Biochemical Characterization of a Lanthanide-Dependent DNAzyme with Normal and Phosphorothioate-Modified Substrates. *Biochemistry* **2015**, *54*, 6132-6138.
33. Liu, S.; Peng, P.; Wang, H.; Shi, L.; Li, T. Thioflavin T binds dimeric parallel-stranded GA-containing non-G-quadruplex DNAs: a general approach to lighting up double-stranded scaffolds. *Nucleic Acids Res.* **2017**, *45*, 12080-12089.
34. Guan, A.-j.; Zhang, X.-F.; Sun, X.; Li, Q.; Xiang, J.-F.; Wang, L.-X.; Lan, L.; Yang, F.-M.; Xu, S.-J.; Guo, X.-M.; Tang, Y.-L. Ethyl-substitutive Thioflavin T as a highly-specific fluorescence probe for detecting G-quadruplex structure. *Scientific Reports* **2018**, *8*, 2666.
35. Renaud de la Faverie, A.; Guédin, A.; Bedrat, A.; Yatsunyk, L.A.; Mergny, J.-L. Thioflavin T as a fluorescence light-up probe for G4 formation. *Nucleic Acids Res.* **2014**, *42*, e65-e65.
36. Zhao, D.; Dong, X.; Jiang, N.; Zhang, D.; Liu, C. Selective recognition of parallel and anti-parallel thrombin-binding aptamer G-quadruplexes by different fluorescent dyes. *Nucleic Acids Res.* **2014**, *42*, 11612-11621.

37. Gao, R.-R.; Yao, T.-M.; Lv, X.-Y.; Zhu, Y.-Y.; Zhang, Y.-W.; Shi, S. Integration of G-quadruplex and DNA-templated Ag NCs for nonarithmetic information processing. *Chem. Sci.* **2017**, *8*, 4211-4222.
38. Luu, K.N.; Phan, A.T.; Kuryavyi, V.; Lacroix, L.; Patel, D.J. Structure of the Human Telomere in K+ Solution: An Intramolecular (3 + 1) G-Quadruplex Scaffold. *J. Am. Chem. Soc.* **2006**, *128*, 9963-9970.
39. Sun, H.; Xiang, J.; Gai, W.; Liu, Y.; Guan, A.; Yang, Q.; Li, Q.; Shang, Q.; Su, H.; Tang, Y.; Xu, G. Quantification of the Na+/K+ ratio based on the different response of a newly identified G-quadruplex to Na+ and K+. *Chemical Communications* **2013**, *49*, 4510-4512.
40. Barnwal, R.P.; Yang, F.; Varani, G. Applications of NMR to structure determination of RNAs large and small. *Arch. Biochem. Biophys.* **2017**, *628*, 42-56.
41. Fürtig, B.; Richter, C.; Wöhnert, J.; Schwalbe, H. NMR Spectroscopy of RNA. *ChemBioChem* **2003**, *4*, 936-962.
42. Patel, D.J.; Shapiro, L.; Hare, D. DNA and RNA: NMR studies of conformations and dynamics in solution. *Quarterly Reviews of Biophysics* **1987**, *20*, 35-112.
43. Tseng, Y.-Y.; Chou, S.-H. Systematic NMR Assignments of DNA Exchangeable Protons. *J. Chin. Chem. Soc.* **1999**, *46*, 699-706.
44. Blancafort, P.; Steinberg, S.V.; Paquin, B.; Klinck, R.; Scott, J.K.; Cedergren, R. The recognition of a noncanonical RNA base pair by a zinc finger protein. *Chemistry & Biology* **1999**, *6*, 585-597.
45. Amrane, S.; Adrian, M.; Heddi, B.; Serero, A.; Nicolas, A.; Mergny, J.-L.; Phan, A.T. Formation of Pearl-Necklace Monomorphic G-Quadruplexes in the Human CEB25 Minisatellite. *J. Am. Chem. Soc.* **2012**, *134*, 5807-5816.
46. Phan, A.T.; Modi, Y.S.; Patel, D.J. Two-repeat Tetrahymena Telomeric d(TGGGGTTGGGGT) Sequence Interconverts Between Asymmetric Dimeric G-quadruplexes in Solution. *J. Mol. Biol.* **2004**, *338*, 93-102.
47. Mao, X.-a.; Marky, L.A.; Gmeiner, W.H. NMR Structure of the Thrombin-Binding DNA Aptamer Stabilized by Sr2+. *J. Biomol. Struct. Dyn.* **2004**, *22*, 25-33.
48. Feigon, J.; Koshlap, K.M.; Smith, F.W. [10]1H NMR spectroscopy of DNA triplexes and quadruplexes. In *Methods Enzymol.*; Academic Press: 1995; Vol. 261, pp. 225-255.
49. Meyer, M.; Hocquet, A.; Sühnel, J. Interaction of sodium and potassium ions with sandwiched cytosine-, guanine-, thymine-, and uracil-base tetrads. *J. Comput. Chem.* **2005**, *26*, 352-364.
50. Hardin, C.C.; Watson, T.; Corregan, M.; Bailey, C. Cation-dependent transition between the quadruplex and Watson-Crick hairpin forms of d(CGCG3GCG). *Biochemistry* **1992**, *31*, 833-841.
51. Smith, F.W.; Feigon, J. Strand orientation in the DNA quadruplex formed from the Oxytricha telomere repeat oligonucleotide d(G4T4G4) in solution. *Biochemistry* **1993**, *32*, 8682-8692.
52. Bishop, G.R.; Chaires, J.B. Characterization of DNA Structures by Circular Dichroism. *Current Protocols in Nucleic Acid Chemistry* **2002**, *11*, 7.11.11-17.11.18.
53. Vorlíčková, M.; Kejnovská, I.; Bednářová, K.; Renčiuk, D.; Kypr, J. Circular Dichroism Spectroscopy of DNA: From Duplexes to Quadruplexes. *Chirality* **2012**, *24*, 691-698.
54. Kejnovská, I.; Renciuk, D.; Palacky, J.; Vorlickova, M. CD Study of the G-Quadruplex Conformation. In *Methods in Molecular Biology*; Yang, D.; Lin, C., Eds.; Springer: 2019; Vol. 2035, pp. 25-44.
55. del Villar-Guerra, R.; Trent, J.O.; Chaires, J.B. G-Quadruplex Secondary Structure Obtained from Circular Dichroism Spectroscopy. *Angew. Chem. Int. Ed.* **2018**, *57*, 7171-7175.
56. Mammana, A.; Carroll, G.; Feringa, B. Circular Dichroism of Dynamic Systems: Switching Molecular and Supramolecular Chirality. In *Comprehensive Chiroptical Spectroscopy: Applications in Stereochemical Analysis of Synthetic Compounds, Natural Products, and Biomolecules*; Berova, N.; Polavarapu, P. L.; Nakanishi, K.; Woody, R. W., Eds.; John Wiley & Sons, Inc.: 2012; pp. 289-316.

57. Sklenář, V.; Tschudin, R.; Bax, A. Water suppression using a combination of hard and soft pulses. *Journal of Magnetic Resonance* **1987**, *75*, 352-357.
58. Hoult, D.I. Solvent peak saturation with single phase and quadrature fourier transformation. *Journal of Magnetic Resonance* **1976**, *21*, 337-347.
59. Briand, J.; Ernst, R.R. Computer-optimized homonuclear TOCSY experiments with suppression of cross relaxation. *Chem. Phys. Lett.* **1991**, *185*, 276-285.
60. Marion, D.; Driscoll, P.C.; Kay, L.E.; Wingfield, P.T.; Bax, A.; Gronenborn, A.M.; Clore, G.M. Overcoming the overlap problem in the assignment of proton NMR spectra of larger proteins by use of three-dimensional heteronuclear proton-nitrogen-15 Hartmann-Hahn-multiple quantum coherence and nuclear Overhauser-multiple quantum coherence spectroscopy: application to interleukin 1.beta. *Biochemistry* **1989**, *28*, 6150-6156.